TECHNICAL REPORT RL-80-11

APERTURE ANALYSIS OF LASER SPECKLE INTERFEROGRAMS

John A. Schaeffel, Jr.
Ground Equipment and Missile Structures Directorate
US Army Missile Laboratory

26 August 1980

Approved for public release; distribution unlimited

U.S. ARMY MISSILE COMMAND
Redstone Arsenal, Alabama 35809

DISPOSITION INSTRUCTIONS

DESTROY THIS REPORT WHEN IT IS NO LONGER NEEDED. DO NOT RETURN IT TO THE ORIGINATOR.

DISCLAIMER

THE FINDINGS IN THIS REPORT ARE NOT TO BE CONSTRUED AS AN OFFICIAL DEPARTMENT OF THE ARMY POSITION UNLESS SO DESIGNATED BY OTHER AUTHORIZED DOCUMENTS.

TRADE NAMES

USE OF TRADE NAMES OR MANUFACTURERS IN THIS REPORT DOES NOT CONSTITUTE AN OFFICIAL INDORSEMENT OR APPROVAL OF THE USE OF SUCH COMMERCIAL HARDWARE OR SOFTWARE.

UNCLASSIFIED

SECURITY CLASSIFICATION OF THIS PAGE *(When Date Entered)*

REPORT DOCUMENTATION PAGE

READ INSTRUCTIONS BEFORE COMPLETING FORM

1. REPORT NUMBER: RL-80-11

2. GOVT ACCESSION NO.

3. RECIPIENT'S CATALOG NUMBER

4. TITLE *(and Subtitle)*: APERTURE ANALYSIS OF LASER SPECKLE INTERFEROGRAMS

5. TYPE OF REPORT & PERIOD COVERED: Technical Report

6. PERFORMING ORG. REPORT NUMBER

7. AUTHOR(s): John A. Schaeffel, Jr.

8. CONTRACT OR GRANT NUMBER(s)

9. PERFORMING ORGANIZATION NAME AND ADDRESS:
Commander
US Army Missile Command
Attn: DRSMI-RL
Redstone Arsenal, Alabama 35898

10. PROGRAM ELEMENT, PROJECT, TASK AREA & WORK UNIT NUMBERS

11. CONTROLLING OFFICE NAME AND ADDRESS:
Commander
US Army Missile Command
Attn: DRSMI-RPT
Redstone Arsenal, Alabama 35898

12. REPORT DATE: 3 Sep 1980

13. NUMBER OF PAGES

14. MONITORING AGENCY NAME & ADDRESS *(if different from Controlling Office)*

15. SECURITY CLASS. *(of this report)*: Unclassified

15a. DECLASSIFICATION/DOWNGRADING SCHEDULE

16. DISTRIBUTION STATEMENT *(of this Report)*

Approved for public release; distribution unlimited

17. DISTRIBUTION STATEMENT *(of the abstract entered in Block 20, if different from Report)*

18. SUPPLEMENTARY NOTES

19. KEY WORDS *(Continue on reverse side if necessary and identify by block number)*

Speckle Interferometry
Displacement Analysis
Nondestructive Testing
Composite Material Testing
Young's Fringes
Computer Aided Fringe Analysis
Flaw Detection
Interferogram Analysis

20. ABSTRACT *(Continue on reverse side if necessary and identify by block number)*

This report documents a new simple system for analyzing laser speckle interferograms for deformation data. In the process the diffracted light from a laser speckle interferogram placed in a collimated light field is selectively mapped into a viewing plane using an aperture. The result is a fringe pattern in the viewing plane which can be easily interpreted for displacement data. The system gives very accurate results.

DD FORM 1 JAN 73 1473 EDITION OF 1 NOV 65 IS OBSOLETE

UNCLASSIFIED

SECURITY CLASSIFICATION OF THIS PAGE *(When Data Entered)*

CONTENTS

ACKNOWLEDGMENT

The author sincerely appreciates the helpful suggestions of Dr. W. F. Swinson from Auburn University and Dr. W. F. Ranson from the University of South Carolina.

1. INTRODUCTION

In recent years several efficient systems have been developed to analyze laser speckle interferograms. These systems employ both single beam and full field reconstruction techniques to perform these analysis. This report documents a new technique for obtaining data using aperture reconstruction. The new technique is one of the most simple and least costly methods to use.

Laser speckle interferograms are most commonly used to make deformation measurements of deformable bodies.[1] Figure 1 illustrates the basic method for making a laser speckle interferogram. When a diffuse surface of a structure is illuminated with coherent radiation, a grainy speckle effect is imaged by the eye or film plane of a camera due to the interference of light from the structure. This speckle effect is enhanced when the structure has microscopic surface irregularities. If the optical configuration remains fixed, the speckle pattern of the test object may be recorded on the film plane of a camera. Further, if the structure is deformed, the speckle points shift with the deformation and a second exposure of the deformed speckle pattern can be made.

Using a technique of double exposure, speckle interferograms of a structure are normally made by photographing the speckle pattern in a deformed and undeformed configuration. A beam of laser light is then passed through a region of the double exposure where the local deformation is desired. As the beam passes through the film, the deformed and undeformed speckle recorded there diffract the laser light and cause an interference effect on a viewing screen. A diffraction halo modulated by light and dark bars of light is produced where the distance 2d between bars is inversely proportional to the distance between the undeformed and deformed speckle on the film plane. A normal to the light and dark bar pattern indicates the axis of deformation of the speckle. The theory to be developed assumes that the deformation region illuminated by the laser beam in reconstruction is uniform and that the linear optical theory is applicable.

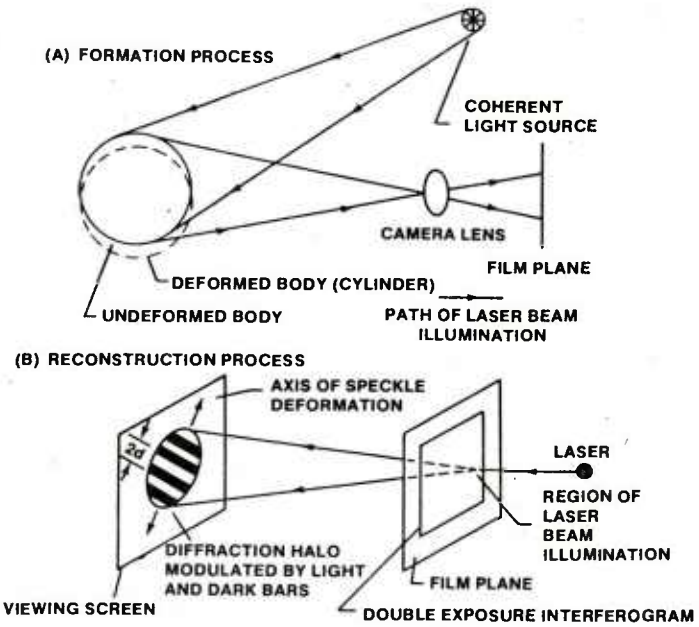

Figure 1. Laser speckle interferometry configuration.

2. THEORETICAL DEVELOPMENT

Figure 2 illustrates the reconstructed diffraction halo modulated by light and dark bars of light. From the linear theory,[1] the displacement in the θ direction of a point on the body is given as:

$$u_\theta = \frac{S\lambda f}{2d} \tag{1}$$

where,

$S \equiv$ film scale factor (magnification ratio).

$\lambda \equiv$ wavelength of laser illumination source.

$f \equiv$ distance from interferogram to analyzer screen.

$d \equiv$ distance from central bright spot to first minima.

$U_\theta \equiv$ displacement of the point illuminated by the laser on the object in the θ direction.

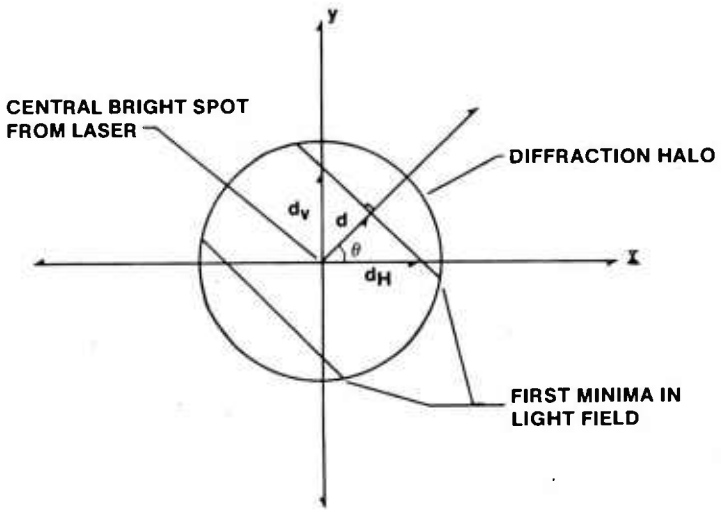

Figure 2. Diffraction halo geometry.

The vertical, U_V and horizontal, U_H components of displacement may be obtained from U_θ as:

$$U_H = U_\theta \cos\theta = \frac{S\lambda f}{2d} \cos\theta \tag{2}$$

$$U_V = U_\theta \sin\theta = \frac{S\lambda f}{2d} \sin\theta \tag{3}$$

and from the geometry,

$$\frac{d}{d_H} = \cos\theta \tag{4}$$

$$\frac{d}{d_V} = \sin\theta \tag{5}$$

therefore,

$$U_H = \frac{S\lambda f}{2d_H} \tag{6}$$

$$U_V = \frac{S\lambda f}{2d_V} \tag{7}$$

Figure 3 illustrates the aperture method for the full field reconstruction of laser speckle interferograms. In this system a laser light source is filtered and collimated to produce a parallel light field. An interferogram is placed in the light field. This action generates an infinite number of Young's fringe diffraction halos. An aperture placed in the diffraction field is used to selectively map only a small region of each diffraction halo into the film plane for photographing purposes. The result in the viewing plane appears as a series of light and dark fringes from which displacements can be obtained. In this process the collimater can also be replaced by a point source of light located at infinity and multiple wavelength light is permissible. The aperture is the key component in the system. Its purpose is to map out small regions in the interferogram plane which interfer in the viewing (or film) plane to produce fringes. In the process, speckle is a deformed configuration and undeformed configuration recorded as a double exposure speckle interferogram, interfer in the viewing plane to produce fringes which can be interpreted for displacements.

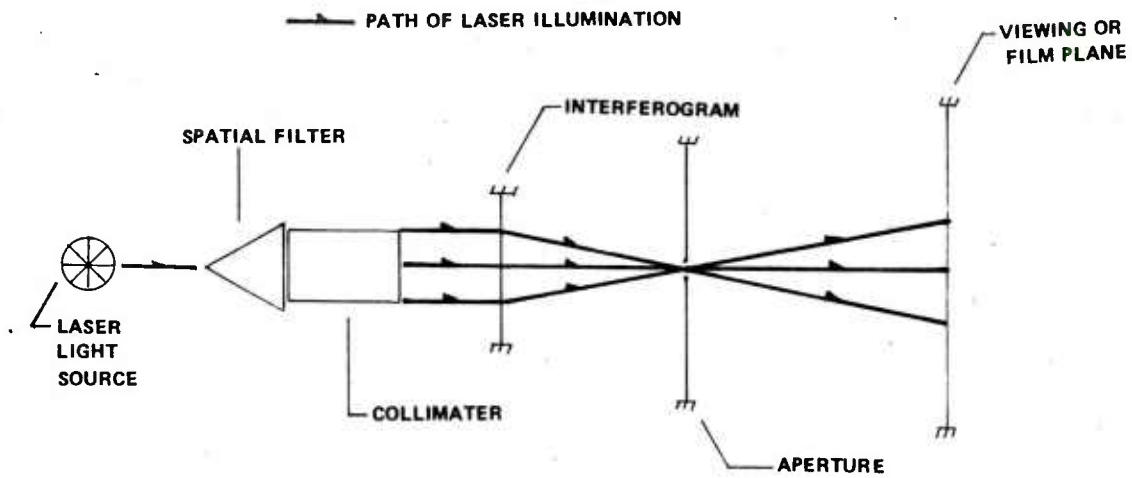

Figure 3. Aperture reconstruction of laser speckle interferograms optical geometry.

A. Optical Path Length Analysis

Figure 4 illustrates the path lengths to be analyzed in this section.

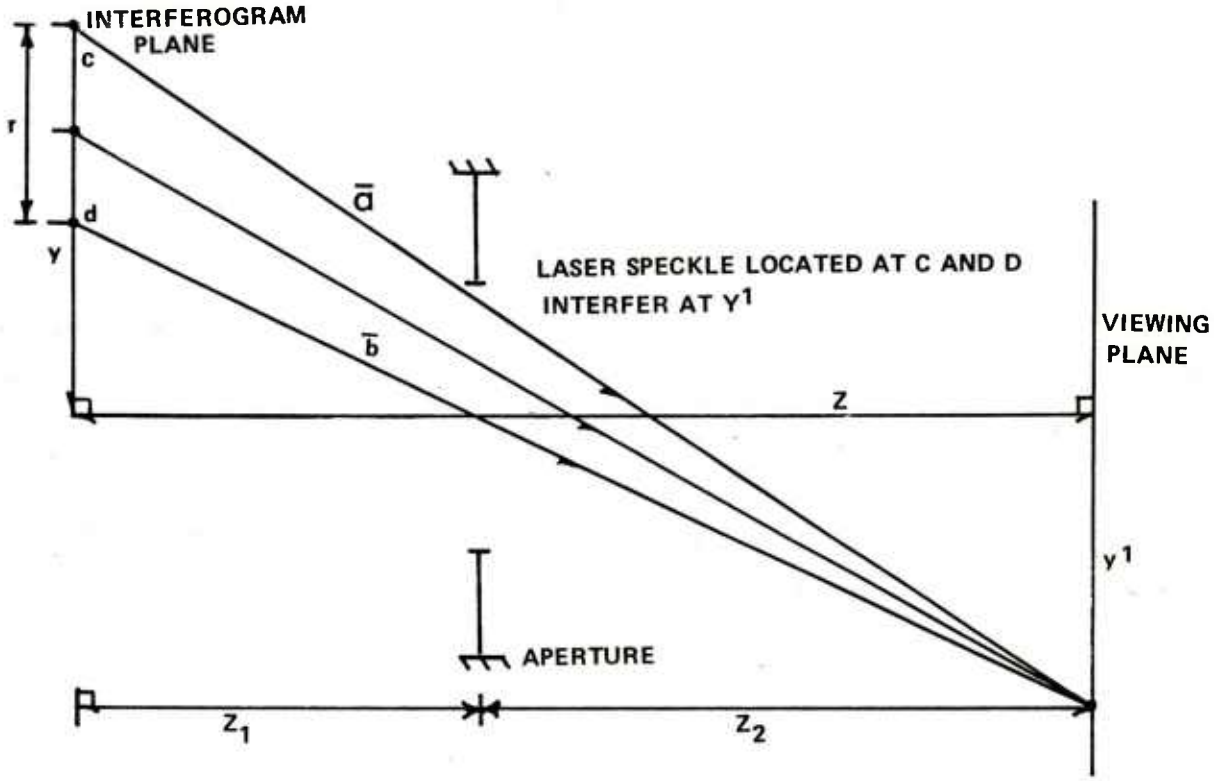

Figure 4. Interference of laser speckle in the viewing plane.

From Figure 4, the path length difference of speckle located at c and d interfering at y^1 is given as[2]:

$$\beta = |\bar{a} - \bar{b}| \tag{8}$$

Now, from the geometry:

$$\beta = \left\{(y + y^1 + \frac{r}{2})^2 + Z^2\right\}^{\frac{1}{2}} - \left\{(y^1 + y - \frac{r}{2})^2 + Z^2\right\}^{\frac{1}{2}} \tag{9}$$

let,

$$\gamma = y + y^1$$

$$\varepsilon = \frac{r}{2}$$

Therefore,

$$\beta = \left\{(\gamma + \varepsilon)^2 + Z^2\right\}^{\frac{1}{2}} - \left\{(\gamma - \varepsilon)^2 + Z^2\right\}^{\frac{1}{2}} \tag{10}$$

For a minima to occur at y^1:

$$\beta = (n + \tfrac{1}{2})\lambda \qquad n = 0,1,2,... \tag{11}$$

For a maxima to occur at y^1:

$$\beta = (n + \tfrac{1}{2})\lambda \qquad n = \tfrac{1}{2}, \tfrac{3}{2}, \tfrac{5}{2}, \ldots \tag{12}$$

For a binomial series[3]:

$$(X + y)^n = X^n + nX^{n-1}y + \frac{n(n-1)}{2!} X^{n-2}y^2 + \frac{n(n-1)(n-2)X^{n-3}y^3}{3!} + \ldots \tag{13}$$

where $(y^2 < X^2)$ (13)

$\overset{o}{oo}$ for $y^2 < X^2$,

$$(X + y)^{\frac{1}{2}} = X^{\frac{1}{2}} + \frac{1}{2}X^{\frac{1}{2}-1}y + \frac{\frac{1}{2}(\frac{1}{2} - 1)X^{\frac{1}{2}-2}y^2}{2.1} + \frac{\frac{1}{2}(\frac{1}{2} - 1)(\frac{1}{2} - 2)\ X^{\frac{1}{2}-3}\ y^3}{3.2.1} + \ldots \tag{14}$$

or, $$(X + y)^{\frac{1}{2}} = X^{\frac{1}{2}} + \frac{1}{2}X^{-\frac{1}{2}}y - \frac{1}{8}X^{-\frac{3}{2}}y^2 + \frac{3}{48}\ X^{-\frac{5}{2}}\ y^3 + \ldots \tag{15}$$

The first and second approximations yield:

$$(X + y)^{\frac{1}{2}} \approx X^{\frac{1}{2}} + \frac{1}{2}\ X^{-\frac{1}{2}}\ y \tag{16}$$

Using the first and second approximations with $Z>>y$ and returning to Equation (9) yields:

$$\beta = \left\{Z + \frac{1}{2}\frac{1}{Z}\ (y + y^1 + \frac{r}{2})^2\right\} - \left\{Z + \frac{1}{2}\frac{1}{Z}\ (y + y^1 - \frac{r}{2})^2\right\}$$

$$= \left\{Z + \frac{1}{2Z}\ (\gamma + \varepsilon)^2\right\} - \left\{Z + \frac{1}{2Z}(\gamma - \varepsilon)^2\right\}$$

$$= \frac{1}{2Z}\left\{(\gamma + \varepsilon)^2 - (\gamma - \varepsilon)^2\right\} = \frac{1}{2Z}\left\{\gamma^2 + 2\gamma\varepsilon + \varepsilon^2 - \gamma^2 + 2\gamma\varepsilon - \varepsilon^2\right\}$$

$$= \frac{1}{2Z}\left\{4\gamma\varepsilon\right\} = \frac{2\gamma\varepsilon}{Z} = \frac{\gamma r}{Z} \tag{17}$$

Now, $Z = Z_1 + Z_2$

$\gamma = y + y^1$

and, $$\frac{y}{Z_1} \cong \frac{y^1}{Z_2} \Rightarrow y = y^1\frac{Z_1}{Z_2} \tag{18}$$

$$\overset{o}{oo}\ \beta = \frac{\gamma r}{Z} = \frac{\left\{y^1 + y^1\frac{Z_1}{Z_2}\right\} r}{Z_1 + Z_2}$$

$$\beta = y^1\left\{\frac{1 + \frac{Z_1}{Z_2}}{Z_1 + Z_2}\right\} r = y^1 \left\{\frac{\frac{Z_2 + Z_1}{Z_2}}{Z_1 + Z_2}\right\} r \tag{19}$$

$$\beta = \frac{y^1 r}{Z_2} = (n + \frac{1}{2})\lambda \tag{20}$$

Finally,

$$r = \frac{SZ_2\lambda}{y_1}(n + \frac{1}{2}) \tag{21}$$

Where,

$r \equiv$ displacement

$y_1 \equiv$ screen location

$\lambda \equiv$ wavelength of light source

$n \equiv$ fringe order

$S \equiv$ interferogram magnification ratio

$Z_2 \equiv$ aperture-viewing plane separation

B. Diffraction Halo Analysis

Figure 5 illustrates an alternate method of analyzing the aperture technique of reconstruction. Consider a diffraction halo originating at y_1 or y_2. The aperture effectively allows only a portion of each halo to be mapped at y_1^1 and y_2^1 respectively. If y_1 or y_2 are minimas then for each minima[1]:

$$r_1 = \frac{S\lambda Z_1}{2y_1} \; ; \; r_2 = \frac{S\lambda Z_1}{\frac{2}{3}y_2} \quad ; \; r_3 = \frac{S\lambda Z_1}{\frac{2}{5}y_3} \tag{22}$$

and so forth, where $r_i^{\cdot}$ defines the order of the minima.

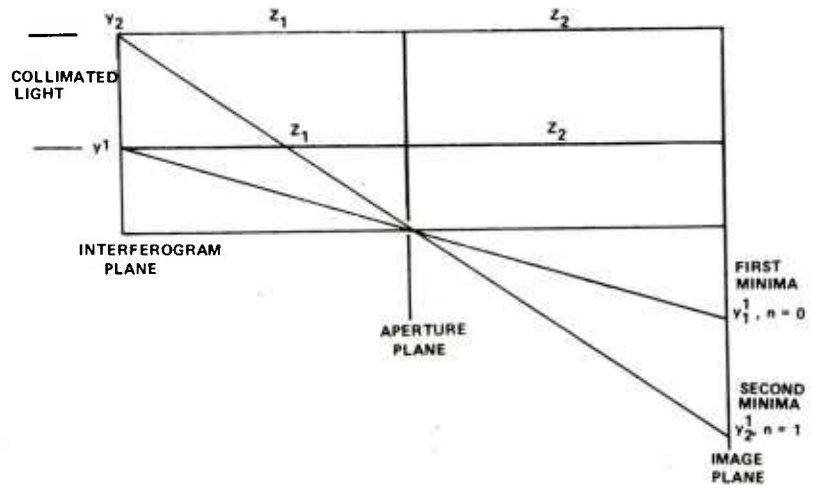

Figure 5. Diffraction halo analysis of the aperture system.

In general, for a minima

$$r = \frac{S\lambda Z_1}{2y}(2n + 1) \quad N = 0, 1, 2, 3,... \tag{23}$$

Now, $$\frac{Z_1}{y} \cong \frac{Z_2}{y'} \tag{24}$$

Therefore,

$$r = \frac{S\lambda Z_2}{2y'}(2n + 1) \tag{25}$$

or, $$r = \frac{S\lambda Z_2}{y'}\left(n + \frac{1}{2}\right) \tag{26}$$

Equation 21 or 26 may be interpreted as follows: Upon viewing the diffraction image in the film plane fringes are assigned the numerical values of N = 0 for the first minima away from the central bright spot. Equations 21 or 26 are used to predict the displacement at a point based upon its distance from the central bright spot and the displacement occurs along an axis formed between the central bright spot and the point of interest.

3. EXPERIMENTAL VERIFICATION

A series of experiments were conducted to verify the theory of Section 2. A typical test is documented in this section for the purpose of comparing aperture and single beam methods of reconstruction. Figure 6 illustrates the laboratory apparatus used in the experiment. The beam from a Spectra Physics Model 125 He-Ne laser (6328Å) was expanded and filtered using a Spectra Physics Model 332 spatial filter. The beam was collimated using a 6.0 inch diameter lense although in some experiments a 2.0 inch beam diameter Spectra Physics Model 336 collimater was used. A Uniblitz Model 310B shutter timer control was used to control the radiation exposure on Poloroid Type 52 film. About a 1.0 sec exposure time was used. The interferogram used in the experiment was obtained by loading an SP250 uniaxial 30° composite specimen in simple tension. The specimen was 0.0625 inch thick by 1.00 inch wide and 12.00 inch long. Figure 7 illustrates typical aperture reconstructions of fringe patterns for similar composite specimens. In Figure 7 the central bright spot was blocked out using a stop in the aperture-film plane field.

Verification of the theory was conducted using the specimen interferogram shown in Figure 8. For the experiment the following test parameters were used:

Z_1 = 13.75 in.

Z_2 = 15.25 in.

$S = (1.14)^{-1}$

f = 131.75 in.

2d = 1.125 in.

$\lambda = 2.4913 \times 10^{-5}$ in.

Aperture diameter = 0.10 in.

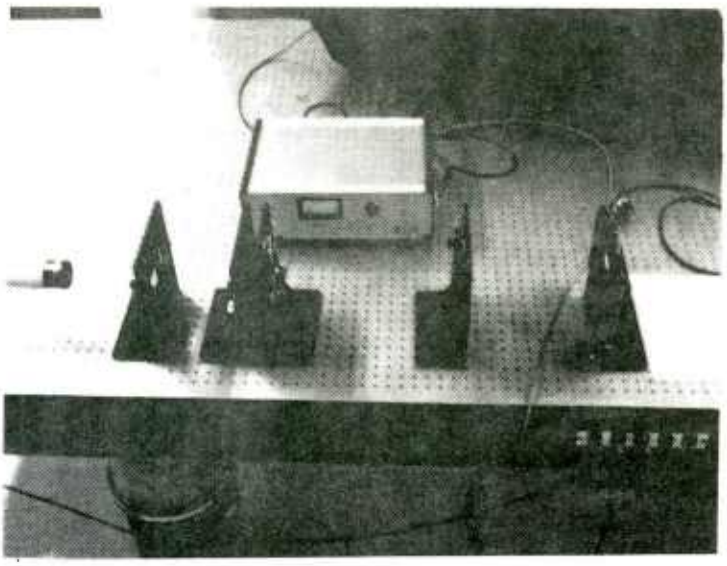

a. System with a commercial collimater.

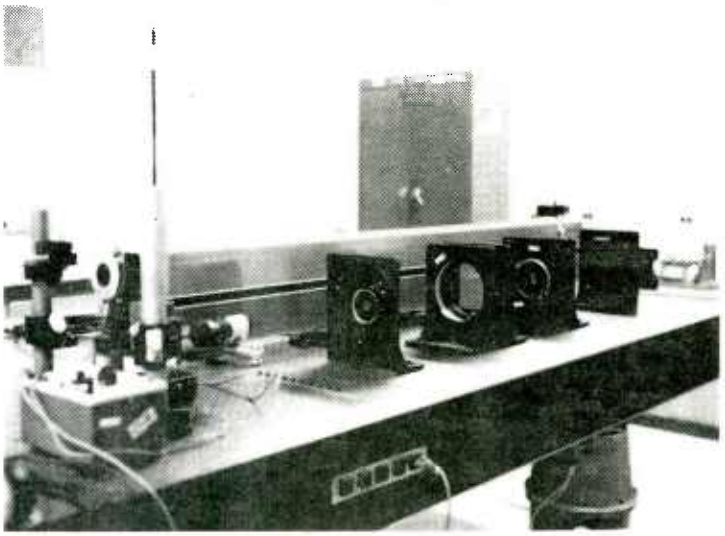

b. System with a lense collimater.

Figure 6. Typical laboratory aperture reconstruction systems.

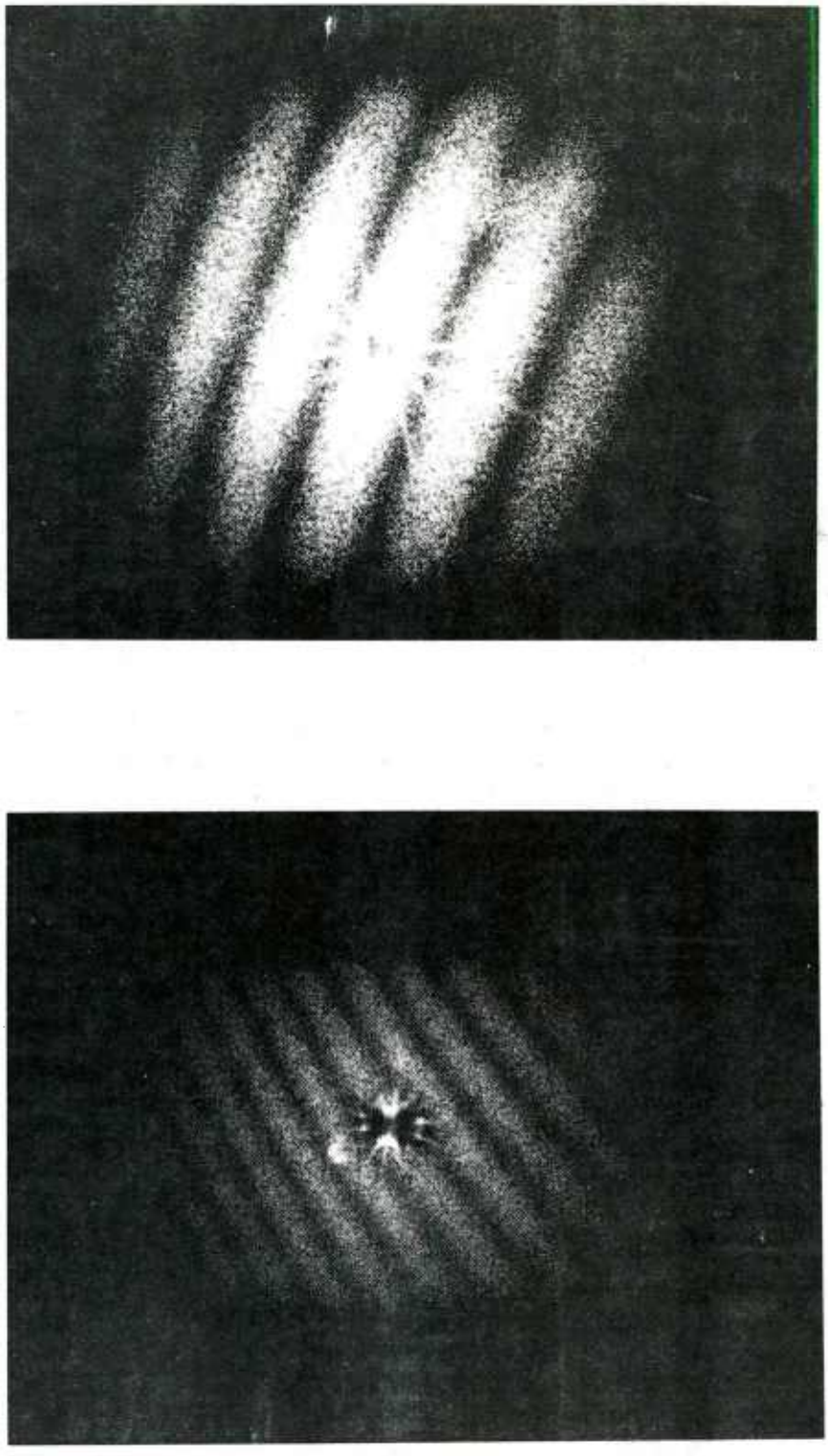

Figure 7. Typical fringe patterns generated from uniaxial composite tensile specimens

In the experiment, data from the aperture reconstruction was compared with the single beam analysis presented in Section 2. Using the single beam analysis:

$$r_{sp} = \frac{S\lambda f}{2D} = (1.14)^{-1} (2.4913 \times 10^{-5}) \frac{(131.75)}{1.125} \text{ in.}$$

$$r_{sp} = 2.5592 \times 10^{-3} \text{ in.}$$

This data was taken at a point equivalent to the central bright spot of Figure 8. Displacement was along the uniaxial load axis.

For comparison purposes using Figure 8 and for n = 3, $y_1^{I} = 0.481$ and $y_1^{II} = 0.436$ along the uniaxial load axis through the central bright spot. For this case using Equation 26, the average displacement becomes:

$$r_A = SZ_2\lambda(n + \tfrac{1}{2}) \frac{\left\{\frac{1}{y_1^{I}} + \frac{1}{y_1^{II}}\right\}}{2} \tag{27}$$

Therefore,

$$r_A = (1.14)^{-1} \frac{(15.25)}{2} (2.4913 \times 10^{-5}) (3 + 0.5) \left\{\frac{1}{.481} + \frac{1}{.436}\right\}$$

$$r_A = 2.5501 \times 10^{-3} \text{ in.}$$

The percent difference between the two solutions is 0.356% indicating excellent agreement in results.

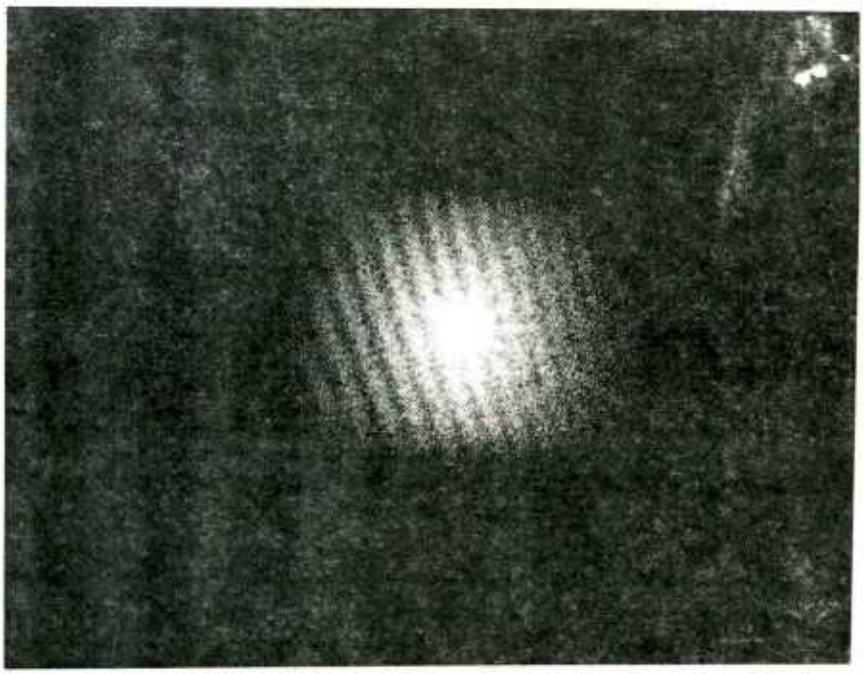

Uniaxial load axis

Figure 8. 30° uniaxial tensile composite specimen used to verify the theory.

4. CONCLUSIONS

The aperture analysis of laser speckle interferograms is a simple direct approach to low-cost quantitative analysis. The process is simple to perform and provides a permanent record of the analysis. Basic advantages of this analysis include:

- Low cost
- Simple optical alignment
- Simple system
- Permanent record of the data
- Excellent fringe contrast
- High signal to noise ratio
- Real time inspection
- Variable sensitivity

The specific disadvantage is that a slight amount of interpretation and formula usage is required. This is so insignificant that it is of little concern.

REFERENCES

1. Mullinix, B.R., Ranson, W.F., Swinson, W.F., and Cost, T.L., Quantification of Flaws in Fibered Composite Structures Using Interferemetric Fringe Patterns, US Army Missile Command, Redstone Arsenal, Alabama, 20 April 1976, Technical Report No. RL-76-18.

2. Klein, Miles V., "Optics," John Wiley & Sons, Inc., New York, 1970.

3. Hodgman, C.D., editor, "Handbook of Chemistry and Physics, 42 Edition," Chemical Rubber Publishing Company, Cleveland, Ohio, 1960.

SYMBOLS

D	Distance from the central bright spot to the first minima
d_H	Horizontal component of d
d_V	Vertical component of d
f	Distance from the interferogram to the analyzer screen
n	Fringe order
r	Displacement in aperture analysis
s	Film scale factor (magnification ratio)
U_H	Horizontal component of Uθ
U_V	Vertical component of Uθ
Uθ	Displacement of the point illuminated by the laser on the object in the θ direction
y^1	Screen location in aperture analysis
Z_2	Aperture to the viewing plane separation
λ	Wavelength of light source
θ	Angle of fringe orientation
β	Optical path length change

DISTRIBUTION

	No. of Copies
Defense Documentation Center Cameron Station Alexandria, Virginia 22314	12
Defense Metals Information Center Battelle Memorial Institute 505 King Avenue Columbus, Ohio 43201	1
Commander US Army Foreign Science and Technology Center Attn: DRXST-SD3 220 Seventh Street, NE. Charlottesville, Virginia 22901	1
Office of Chief of Research and Development Department of the Army Attn: DARD-ARS-P Washington, DC 20301	1
Commander US Army Electronics Command Attn: DRSEL-PA-P -CT-DT -PP, Mr. Sulkolove Fort Monmouth, New Jersey 07703	1 1 1
Commander US Army Natick Laboratories Kansas Street Attn: STSNLT-EQR Natick, Massachusetts 01760	1
Commander US Army Mobility Equipment Research and Development Center Fort Belvoir, Virginia 22060	1
Director USA Mobility Equipment Research and Development Center Coating and Chemical Laboratory Attn: STSFB-CL Aberdeen Proving Ground, Maryland 21005	1
Commander Edgewood Arsenal Attn: SAREA-TS-A Aberdeen Proving Ground, Maryland 21010	1

	No. of Copies
Commander Picatinny Arsenal Attn: SARPA-TS-S, Mr. M. Costello Dover, New Jersey 07801	1
Commander Rock Island Arsenal Research and Development Attn: 9320 Rock Island, Illinois 61201	1
Commander Watervliet Arsenal Watervliet, New York 12189	1
Commander US Army Aviation Systems Command Attn: DRSAV-EE -MT, Mr. Vollmer St. Louis, Missouri 63166	1 1
Commander US Army Aeronautical Depot Maintenance Center (Mail Stop) Corpus Christi, Texas 78403	1
Commander UA Army Test and Evaluation Command Attn: DRSTE-RA Aberdeen Proving Ground, Maryland 21005	1
Commander Attn: STEAP-MT Aberdeen Proving Ground, Maryland 21005	1
Chief Bureau of Naval Weapons Department of the Navy Washington, DC 20390	1
Chief Bureau of Ships Department of the Navy Washington, DC 20315	1
Naval Research Laboratory Attn: Dr. M. M. Krafft Code 8430 Washington, DC 20375	1

	No. of Copies
Commander Wright Air Development Division Attn: ASRC Wright-Patterson AFB, Ohio 45433	1
Director Air Force Materiel Laboratory Attn: AFML-DO-Library Wright-Patterson AFB, Ohio 45433	1
Director Army Materials and Mechanics Research Center Attn: DRXMR-PL -MT, Mr. Farrow Watertown, Massachusetts 02172	1 1
Commander White Sands Missile Range Attn: STEWS-AD-L White Sands Missile Range, New Mexico 88002	1
Jet Propulsion Laboratory California Institute of Technology Attn: Library/Acquisitions 111-113 4800 Oak Grove Drive Pasadena, California 91103	1
Sandia Laboratories Attn: Library P.O. Box 969 Livermore, California 94550	1
Commander US Army Air Defense School Attn: ATSA-CD-MM Fort Bliss, Texas 79916	1
Technical Library Naval Ordnance Station Indian Head, Maryland 20640	1
Commander US Army Materiel Development and Readiness Command Attn: DRCMT Washington, DC 20315	1
Headquarters SAC/NRI (Stinfo Library) Offutt Air Force Base, Nebraska 68113	1

	No. of Copies
Commander Rock Island Arsenal Attn: SARRI-KLPL-Technical Library Rock Island, Illinois 61201	1
Commander (Code 233) Naval Weapons Center Attn: Library Division China Lake, California 93555	1
Department of the Army US Army Research Office Attn: Information Processing Office P.O. Box 12211 Research Triangle Park, North Carolina 27709	1
Commander US Army Research Office Attn: DRXRO-PW, Dr. R. Lontz P.O. Box 12211 Research Triangle Park, North Carolina 27709	2
US Army Research and Standardization Group (Europe) Attn: DRXSN-E-RX, Dr. Alfred K. Nodoluha Box 65 FPO New York 09510	2
Headquarters Department of the Army Office of the DCS for Research Development and Acquisition Room 3A474, The Pentagon Attn: DAMA-ARZ Washington, DC 20310	2
US Army Materiel Systems Analysis Activity Attn: DRXSY-MP Aberdeen Proving Ground, Maryland 21005	1
IIT Research Institute Attn: GACIAC 10 West 35th Street Chicago, Illinois 60616	1
ADTC (DLDSL) Eglin Air Force Base, Florida 32542	1
University of California Los Alamos Scientific Laboratory Attn: Reports Library P.O. Box 1663 Los Alamos, New Mexico 87545	1

	No. of Copies
Commander US Army Materiel Development and Readiness Command Attn: DRCRD DRCDL 5001 Eisenhower Avenue Alexandria, Virginia 22333	 1 1
Director Defense Advanced Research Projects Agency 1400 Wilson Boulevard Arlington, Virginia 22209	 1
DRSMI-LP, Mr. Voigt	1
-R	1
-RL, Mr. Comus	1
-RLA, Mr. Pettey	1
Mr. Schaeffel	50
-RPT (Record Copy)	1
(Reference Copy)	1